Available online at www.sciencedirect.com
SCIENCE DIRECT®
Journal of Power Sources 133 (2004) 169–174
JOURNAL OF POWER SOURCES
www.elsevier.com/locate/jpowsour

Impedance analysis of a disk-type SOFC using doped lanthanum gallate under power generation

Tohru Kato [a], Ken Nozaki [a], Akira Negishi [a], Ken Kato [a], Akihiko Monma [a], Yasuo Kaga [a], Susumu Nagata [a], Kiyonami Takano [a,*], Toru Inagaki [b], Hiroyuki Yoshida [b], Kei Hosoi [c], Koji Hoshino [c], Taner Akbay [c], Jun Akikusa [c]

[a] *Fuel Cell Group, Energy Electronics Institute, AIST, 1-1-1 Umezono Tsukuba-shi, Ibaraki 305-8568, Japan*
[b] *Energy Use R&D Center, The Kansai Electric Power Company Inc., 11-20 Nakoji, 3-Chome, Amagasaki, Hyogo 661-0974, Japan*
[c] *Central Research Institute, Naka Research Center, Mitsubishi Materials Corp., 1002-14 Mukohyama, Naka-machi, Naka-gun, Ibaraki 311-0102, Japan*

Received 17 September 2003; received in revised form 9 February 2004; accepted 10 February 2004

Available online 9 April 2004

Abstract

Impedance measurements were carried out under practical power generation conditions in a disk-type SOFC, which may be utilized as a small-scale power generator. The tested cell was composed of doped lanthanum gallate ($La_{0.8}Sr_{0.2}Ga_{0.8}Mg_{0.15}Co_{0.05}O_{3-\delta}$) as the electrolyte, $Sm_{0.5}Sr_{0.5}CoO_3$ as the cathode electrode and $Ni/Ce_{0.8}Sm_{0.2}O_2$ cermet as the anode electrode. The cell impedance was measured between 10 mHz and 10 kHz by varying the fuel utilization and gas flow rate and plotted in complex impedance diagrams. The observed impedance shows a large semi-circular pattern on the low frequency side. The semi-circular impedance, having a noticeably low characteristic frequency between 0.13 and 0.4 Hz, comes from the change in gas composition, originally caused by the cell reaction. The change in impedance with the fuel utilization (load current) and the gas flow rate agreed qualitatively well with the theoretical predictions from a simulation. This impedance was dominant under high fuel-utilization power-generation conditions. The impedance, which described the activation polarizations in the electrode reactions, was comparatively small and scarcely changed with the change in fuel utilization (load current) and gas flow rate.

Keywords: Disk-type SOFC; Doped lanthanum gallate; Impedance analysis; Power generation; Gas conversion impedance

1. Introduction

The impedance analysis method has been utilized quite frequently in the research and development of solid oxide fuel cells (SOFCs). However, in the published literature, there are limited numbers of impedance measurements under practical power generation conditions, such as high fuel utilization, e.g. 70–80% or above. The main reason for this may be because the measurement and the interpretation of the impedance data are rather difficult in a full-scale cell. It is expected that the equivalent circuit of impedance under power generation conditions would be useful for the performance simulation, design and evaluation of the cell. Previously, the relationship between the total cell impedance and the impedance of the local cell in a disk-type SOFC was theoretically examined using the numerical simulation reported elsewhere [1].

In this study, in order to examine the possibility of an AC impedance analysis to evaluate cell performance, the total cell impedance was measured by changing the fuel utilization and the gas flow rate under actual power generation conditions in a disk-type SOFC. Furthermore, a complete discussion was provided in comparison with previous theoretical simulation results.

2. Experimental procedure

The impedance was measured in a disk-type SOFC made of the doped lanthanum gallate electrolyte developed by Ishihara et al. [2,3]. Currently, the complete system is under joint development by the Mitsubishi Materials Corp. [4,5] and The Kansai Electric Power Company Inc. [6]. A schematic diagram of the test cell is shown in

* Corresponding author. Tel.: +81-298-61-5794; fax: +81-298-61-5805.
E-mail address: k.takano@aist.go.jp (K. Takano).

0378-7753/$ – see front matter © 2004 Elsevier B.V. All rights reserved.
doi:10.1016/j.jpowsour.2004.02.010

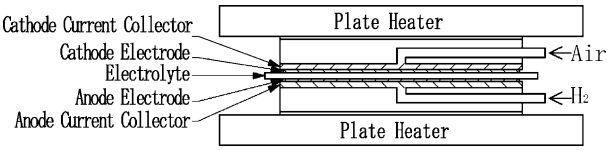

Fig. 1. Schematic diagram of a disk-type SOFC.

Fig. 1. It consists of a composite disk made of a solid electrolyte and electrodes, structured current collectors and metal separators for the anode and cathode. Fuel gas and air radially flow through the structured current collectors. The self supporting electrolyte disk, made of $La_{0.8}Sr_{0.2}Ga_{0.8}Mg_{0.15}Co_{0.05}O_{3-\delta}$, as reported previously [4], has a 100 mm outer diameter and about a 200 μm thickness. The electrochemically active cell is formed by co-firing the electrolyte together with the screen-printed $Sm_{0.5}Sr_{0.5}CoO_3$ cathode and $Ni/Ce_{0.8}Sm_{0.2}O_2$ cermet anode. The effective electrode diameter is 85 mm (56.75 cm^2). The cell made in this way was thermally and electrochemically stable, and it was proved that the cell operated stably for a long duration [5,6] (more than 1600 h).

For the measurement of the impedance, a sinusoidal current superimposed as a small alternating current on a load current was applied using Solartron 1255 and 1287 instruments as a function generator and a galvanostat, respectively. The frequency range for the alternating current was from 10 kHz to 10 mHz. The AC current through the cell was detected using a current probe (Hioki3274). The potential difference between the current correctors and the current signal were recorded by a digital recorder (Yokogawa DL708E), and analyzed using the Fourier transform to obtain impedances after the measurement.

Pure hydrogen was used as the fuel and dry air as the oxidant. The air flow rate was five times the hydrogen flow rate. The standard experimental conditions were a hydrogen flow rate of 170 ml/min, an air flow rate of 850 ml/min, and a load current of 17.0 A. The impedance data were measured by varying the load current at a fixed flow rate and also by varying the flow rate at a fixed load current. During these measurements, the cell temperature was monitored in both structured current collectors using sheathed thermocouples. Throughout the tests, the temperature profiles on the anode and cathode sides remained almost identical at 1018 ± 2 K.

3. Results and discussion

At the standard flow rate and load current (170 ml/min, 17.0 A), the impedance was measured three times at the beginning of the experiment, the middle and the end, and the obtained Cole–Cole plots of the cell impedance between the anode and cathode are shown in Fig. 2. The plots indicated that the impedance increased during the experiment, especially more increased during the initial runs. This increase seemed to be caused by the initial stabilizing process of the

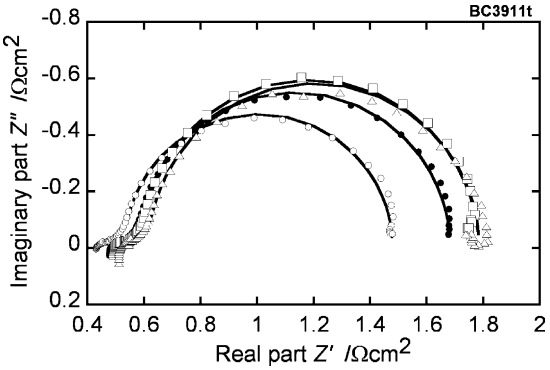

Fig. 2. Cole–Cole plots of the total cell impedance obtained at the standard flow rate (H_2: 170 ml/min) and load current (17.0 A) at the beginning of the experiment (○), the middle (□) and the end (△), and the averaged values (●). Symbols indicate experimental and (—) fitting results using the equivalent circuit (Fig. 7).

cell system, because the cell performance then stabilized. This increase is considered in the following discussion on the experimental results.

Fig. 3 shows the Cole–Cole plots of the cell impedance measured by changing the load current at the standard flow rate. The change in the DC cell terminal voltage versus the load current during this measurement is shown in Fig. 4. Fig. 5 shows the Cole–Cole plots of the cell impedance measured by changing the flow rates at the standard load current. The Cole–Cole plots for the standard flow rate and load current are shown as the average of Fig. 2 in order to avoid any complication. Through the impedance in the figures are the impedance between the current correctors of the anode and cathode, we also measured the impedance between the anode current corrector and the reference electrode, and between the cathode current corrector and the reference elec-

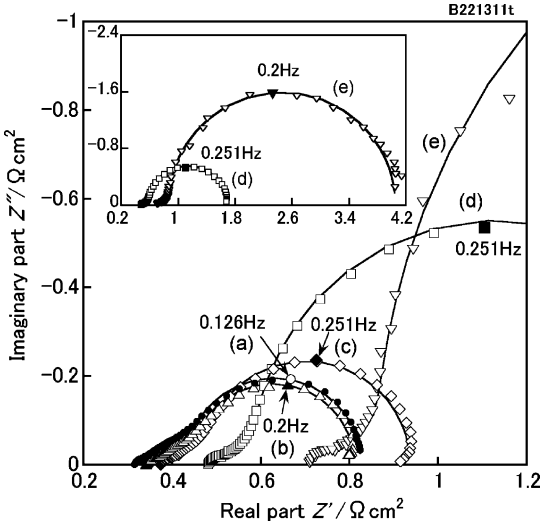

Fig. 3. Impedance Cole–Cole plots at a fixed flow rate (H_2: 170 ml/min) at 1018 K with the fuel utilization parameter (load current): (a) 4.1% (1.0 A); (b) 23.3% (5.67 A); (c) 46.5% (11.35 A); (d) 69.8% (17.0 A); (e) 80.0% (19.5 A). Symbols indicate experimental and (—) fitting results using an equivalent circuit (Fig. 7).

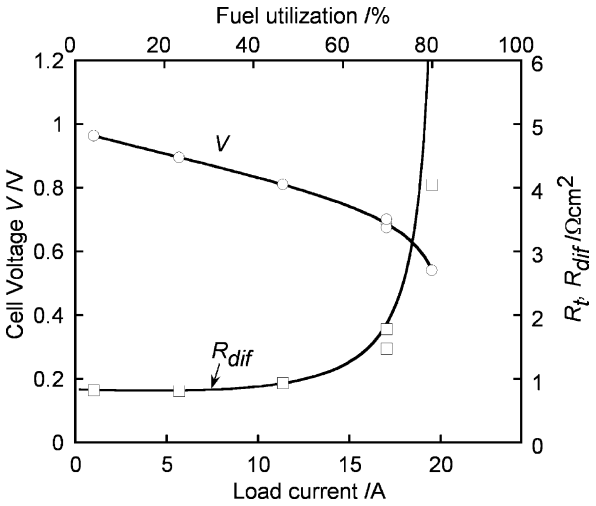

Fig. 4. Cell voltage vs. load current at the impedance measurement in Fig. 3 accompanying the real part resistance at 10 mHz, R_t (□), and the differential resistance, R_{dif} (—), which was calculated from the derivative of the curve fitted to the *V–I* characteristics with current.

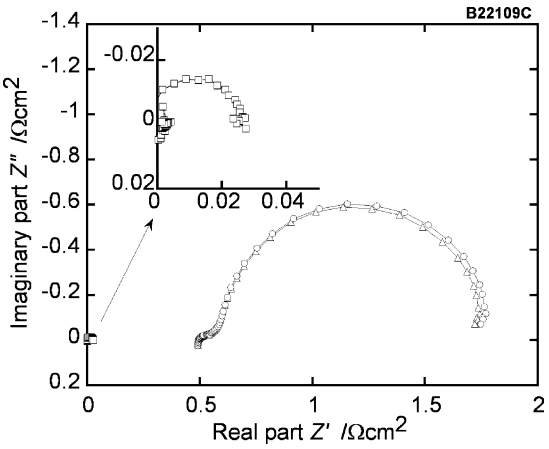

Fig. 6. Cole–Cole plots of the impedances between respective electrodes at the standard fixed flow rate and load current. (○) Between anode and cathode; (□) between anode and reference electrode; (△) between cathode and reference electrode.

trode using a reference electrode made of a platinum mesh placed on the cathode side of the electrolyte outside the electrode. Fig. 6 shows the measured impedance between the respective electrodes under standard conditions. The figure indicates that the impedance between the cathode and the reference electrode was extremely small in comparison with that between the anode and the reference electrode. Through there is an uncertainty in the position at which the electrical potential the reference electrode is referring to between the anode and the cathode, an especially large uncertainty in the large size cell, the total cell impedances between anode and cathode discussed in this paper seem to mainly reflect impedance of the anode.

The Cole–Cole plots seem to consist of the sum of a number of small semicircles between several Hertz and 10 kHz and a large semicircle with a characteristic frequency of about 0.13–0.4 Hz as the maximum of the imaginary part of the impedance. Also, an inductive behavior was observed at

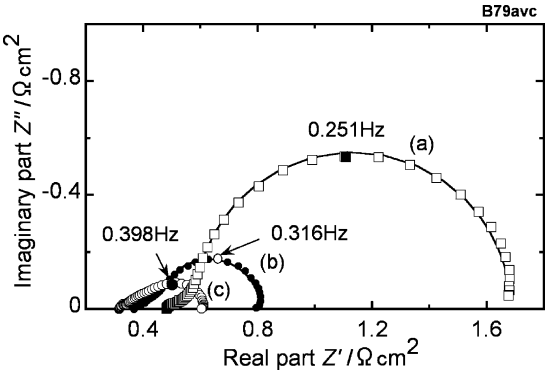

Fig. 5. Impedance Cole–Cole plots at a fixed load current (17.0 A) at 1018 K with the parameter of H_2 flow rate: (a) 170 ml/min; (b) 235 ml/min; (c) 395 ml/min. Symbols indicate experimental and (—) fitting results using an equivalent circuit (Fig. 7).

the high and low frequency edges. The trend at the high frequency edge was due to the inductance of the measurement system. The inductive behavior, as the impedance decreased with a decrease in frequency near the low frequency edge, does not appear in the usual electrode reaction. Though the cause of the inductive impedance was not clarified in our case, the observed inductive behavior is noteworthy. Such an impedance behavior on the air side electrode in the SOFC was also reported in other papers [7,8].

Fig. 3 also shows the real part resistance, R_t, at the low frequency edge (10 mHz) and the differential resistance, R_{dif}, which was calculated from the derivative of the curve fitted to the *V–I* characteristics with current. Both resistances agreed very well up to the point of the highest fuel utilization, where a derivative of the curve had the highest uncertainty. In other words, the measured impedance indicates the derivative of the dc *V–I* characteristics curve at a sufficiently low frequency.

A numerical simulation of a disk-type SOFC for impedance analysis has been reported [1], in which the simulation relates the impedance of the local cell to the whole cell impedance by solving an unsteady molar transport quasi-one-dimensional flow problem, considering that the concentration distributions of the chemical species change due to the cell reaction with the gas flow, resulting in a change in the distributions of the electromotive force and current. According to this simulation study, Cole–Cole plots for the total cell impedance on a disk-type SOFC show a capacitive semicircle, even if the impedance of the local cell is assumed to be an ohmic resistance for simplicity through it may be a complex number including the *RC* parallel circuit which is related to the electrode reaction and diffusion, etc. This impedance semicircle originates from the electromotive force change due to the current with the cell reaction, where hydrogen gas is converted to water vapor in the fuel flow, and oxygen gas in the oxidizing

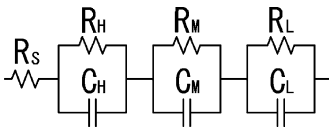

Fig. 7. The equivalent circuit for fitting the measured impedance.

agent flow is consumed. The mechanism of the impedance is the same as that of the gas conversion impedance introduced for a perfect mixing ideal anode by Primdahl and Mogensen [9]. The appearance of the impedance discussed here is inevitable if you wish to operate an SOFC with high energy conversion efficiency which requires a high fuel utilization. Hence, the impedance could be reduced by supplying a large amount of fuel only if you had no further concern about energy conversion efficiency. The characteristic time for this impedance is the period during which the fuel gas passes through the cell because the reaction of the flowing gas occurs during this period. Therefore, the characteristic frequency is inversely proportional to the flow rate, resulting in a relatively low characteristic frequency.

It was considered that there were two other possible impedances with a semicircle diagram related to the gas transfer process in the tested cell. One is the impedance related to the finite-length diffusion of chemical species in the gas flow channels of fuel and air and the other is that in the porous electrodes. They could be expressed as the Warburg impedance in the finite-length diffusion. The characteristic frequency of the semicircle that the Warburg impedance made in the finite-length diffusion was roughly estimated to be over several Hz at least for the porous electrodes and over several 10 Hz for the gas flow channels. These frequencies are much higher by over one order than the characteristic frequency of the low frequency semicircle impedance in Figs. 3 and 5.

For a further discussion, the parameter fitting the experimental results was done using the equivalent circuit shown in Fig. 7, which consisted of three *RC* parallel circuits and a resistance, R_S. The first two *RC* parallel circuits may correspond to the electrode impedances consisting of the interfacial capacitances between the electrode and electrolyte and the reaction resistances on the anode and the cathode, trough the resistance on the cathode may be small in comparison with the other, and possibly to the impedances related to the finite-length diffusions. The third one is the impedance related to the gas conversion as mentioned above. The subscripts of the circuit element parameters, H, M and L are acronyms for high, middle and low characteristic frequencies, respectively. It is considered that R_S consists of the electrolyte resistance, the electrode material resistances for the anode and cathode, and the contact resistances between the electrodes and current collectors.

Fitting the results by the above-mentioned equivalent circuit is shown by the solid lines in Figs. 2, 3 and 5. There is good agreement in the low frequency region except for the

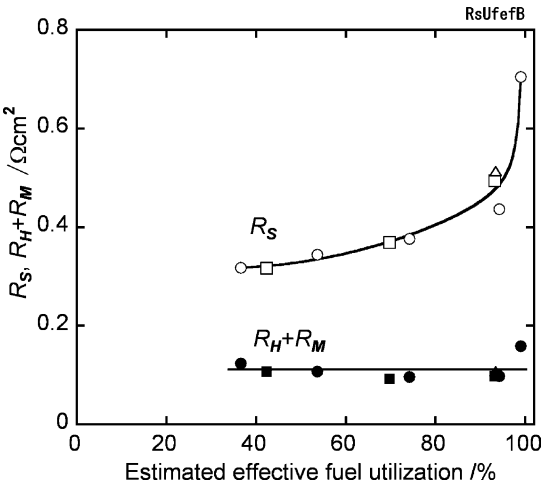

Fig. 8. R_S (open symbols) and $R_H + R_M$ (solid symbols) vs. the estimated effective fuel utilization. Circle, square and triangle at the standard conditions (effective fuel utilization about 92%) were obtained from the three measurements at the beginning of the experiment, the middle and the end, respectively; the other circles were obtained from the experimental data in Fig. 3; the other squares were obtained from the experimental data in Fig. 5.

inductive impedance near the low frequency edge. The capacitance for the low frequency semicircles was calculated to vary from 0.3 to 3 F/cm^2, and it is considered that such a large capacitance may not originate from the interface layer. Thus, the impedance of the low frequency semicircle might be related to the gas conversion. The high and intermediate frequency semicircles, which might be related to the electrode reaction and the finite-length diffusion, were relatively small.

Because the gas conversion impedance depends on the partial pressure of the chemical species [9], it is necessary to evaluate the impedance against the effective fuel utilization, considering the gas composition change caused by the current due to the electronic conduction in the mixed conductive electrolyte, such as the doped lanthanum gallate electrolyte. [1] Therefore, in Figs. 8 and 9 R_S, $R_H + R_M$ and R_L, which were obtained by the fitting, are shown vs. the effective fuel utilization, which was estimated by making the following assumptions. Effective fuel utilization was assumed to be 99% at a load current of 19.5 A, which was nearly the output limit at the standard flow rate, and the internal current by electronic conduction was proportional to the terminal voltage by assuming a constant electronic conductivity. With this assumption, the electronic conduction was evaluated to be about 3% of the total conductivity, while the ionic transport number of the identical electrolyte was reported previously to be 95–97% [4].

In Figs. 8 and 9, R_S, $R_H + R_M$ and R_L for the three measurements at the beginning, the middle and the end of the experiment are denoted by the circle, square and triangle symbols, respectively. It was indicated that the impedance increased during the experiment but the increase was not big enough to change the trends in the experimental results.

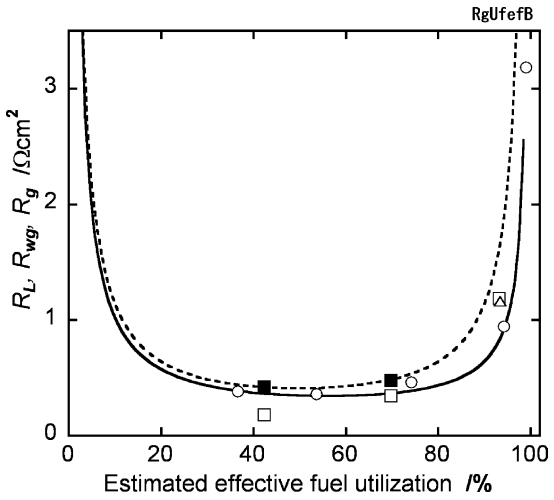

Fig. 9. R_L (Symbols) vs. effective fuel utilization accompanying the gas conversion impedance, R_g (broken line), from Primdahl and Mogensen [9] and whole cell gas conversion impedance, R_{wg} (solid line), from simulation results by Takano et al. [1]. Circle, square and triangle at the standard conditions (effective fuel utilization about 92%) were obtained from the three measurements at the beginning of the experiment, the middle and the end, respectively; (other circle) R_L obtained from Fig. 3; (other square) R_L obtained from Fig. 5; (solid square) normalized R_L by the ratio of fuel gas flow rate.

According to the simulation [1], the resistance at a sufficiently high frequency is not affected by the non-uniformity in the current distribution and by the fuel utilization, provided that the local cell resistance does not change. However, R_S increased from 0.3 to 0.7 Ω cm^2 with the increase in the fuel utilization. As mentioned above, it is considered that R_S consists of the electrolyte resistance, electrode material resistances for the anode and cathode, and contact resistances between the electrodes and current collectors. The conductivity of the electrolyte used in this study is about 0.1 S/cm at 1018 K [4], and the resistance of the electrolyte for a 200 μm thickness is about 0.2 Ω cm^2. Because the electrolyte resistance does not change with the oxygen partial pressure as reported by Ishihara et al. [10], it does not change with the fuel utilization. None of the resistances mentioned above explains the increase in R_S with the increase in fuel utilization. The resistance of the interfacial layer, which may have been formed between the cathode and electrolyte during the co-firing process, also cannot explain the shift in R_S, because the change in the atmospheric oxygen partial pressure over the cathode is relatively small due to the low oxygen utilization. On the other hand, the possible interfacial zone between the anode and electrolyte might be the cause of the shift in R_S, because the change in the oxygen partial pressure over the anode is quite large under the experimental conditions. A further investigation is needed for the complete elucidation of the change in R_S.

$R_H + R_M$, which might be related to reaction resistance on the anode and cathode and the finite-length diffusion, was comparatively small at 0.1 Ω cm^2 and almost constant regardless of the fuel utilization and gas flow rate.

The resistance, R_{wg}, for the total cell impedance related to the gas conversion given by the simulation from Takano et al. [1] and the resistance, R_g, for the gas conversion impedance given by the equation from Primdahl and Mogensen [9] as well as R_L are shown in Fig. 9. When the fuel utilization increased at a fixed gas flow rate, R_L decreased with an increase in the effective fuel utilization from 36.5 to 53.6%. R_L increased with a further increase in fuel utilization and then reached a very high value near the output limit. Such a change in R_L agrees well with the changes in R_{wg} and R_g. Such a change in R_{wg} and R_g is explained as follows. These impedances are the coefficients which describe the electromotive force change due to the current in the electrochemical reaction. The electromotive force change due to the current comes from the partial pressure changes in hydrogen, water and oxygen in the cell. The partial pressure change due to a certain amount of electrochemical reaction (kinetic current) becomes greater at lower partial pressures. At a lower fuel utilization, the electromotive force change becomes greater due to the greater change in the water partial pressure because of the lower water partial pressure, while it also becomes greater by the greater change in the hydrogen partial pressure because of the lower hydrogen partial pressure at the higher fuel utilization. R_{wg} and R_g then have higher values as the fuel utilization approaches 0 or 100%, and they have minimum values around the midpoint of the fuel utilization, where the partial pressures of water and hydrogen are great. R_{wg} also includes the influence of the change in the oxygen partial pressure on the cathode, and the convolution of these phenomena appears as the gas conversion impedance of the whole cell.

By changing the gas flow rate at a fixed load current, R_L deviated from the curve of the standard flow rate. Because the gas conversion impedance is inversely proportional to the gas flow rate [9], R_L was normalized by the gas flow rate to the standard flow rate. The normalized R_L agreed rather well with R_{wg} of the standard flow rate, as shown in Fig. 9.

The characteristic frequency of the low frequency semicircle first increased to about 0.25 Hz with an increase in the fuel utilization at the standard flow rate and then decreased with a further increase in the fuel utilization (Fig. 3). The transit period of fuel gas passing through the cell was about 0.53 s at the standard flow rate. The characteristic frequency calculated as $(1/2\pi\tau)$ was about 0.3 Hz, where τ is the characteristic time. However, according to the simulation, the characteristic frequency increases to 0.4 Hz at a 50% fuel utilization because of the influence by the oxidant gas flow. Also, the characteristic time increases and the characteristic frequency decreases as the fuel utilization approaches 0 or 100% [1]. The characteristic frequencies of the simulation were on the same order as that of the experimental values. The tendency with the fuel utilization agreed well with the experimental observations (Fig. 3). The transit period is inversely proportional to the gas flow rate, and

the characteristic frequency increases with the gas flow rate. Such a change in the frequency also well agrees with the experimental findings (Fig. 5).

Based on the above discussion, it is concluded that the impedance of the low frequency semicircle is dominant under practical power generation conditions and that it is mainly due to the gas conversion during the cell reaction.

4. Concluding remarks

In a relatively large-size disk-type SOFC using doped lanthanum gallate as the electrolyte, impedance measurements were carried out under practical power generation conditions and the following conclusions were obtained.

The observed impedance shows a large semi-circular pattern on the low frequency side. The semi-circular impedance, having a noticeably low characteristic frequency between 0.13 and 0.4 Hz, comes from the change in the gas composition, originally caused by the cell reaction. The change in this impedance with the fuel utilization (load current) and gas flow rate qualitatively agreed with the theoretical predictions from the simulation. This impedance is also found to be dominant under high-efficiency power generation conditions.

The impedance of the multi semicircles between several Hertz and 10 kHz, which might be related to the electrode reaction and the finite-length diffusion, was comparatively small and scarcely changed with the changing fuel utilization and gas flow rate.

The resistance at 10 kHz increased with an increase in the fuel utilization. None of the ohmic resistances so far reported seem to provide a reasonable explanation, suggesting the necessity of further investigations.

References

[1] K. Takano, S. Nagata, K. Nozaki, A. Monma, T. Kato, Y. Kaga, A. Negishi, K. Kato, T. Inagaki, H. Yoshida, K. Hosoi, K. Hoshino, T. Akbay, J. Akikusa, Numerical simulation of a disk type SOFC for impedance analysis under power generation, J. Power Sources 132 (1–2) (2004) 42–51.
[2] T. Ishihara, H. Matsuda, Y. Takita, J. Am. Chem. Soc. 116 (1994) 3801.
[3] T. Ishihara, et al., Chem. Mater. 11 (8) (1999) 2081–2088.
[4] K. Kuroda, I. Hashimoto, K. Adachi, J. Akikusa, Y. Tamou, N. Komada, T. Ishihara, Y. Takita, Solid State Ionics 132 (2000) 199–208.
[5] J. Akikusa, K. Adachi, K. Hoshino, T. Ishihara, Y. Takita, J. Electrochem. Soc. 148 (11) (2001) A1275–A1278.
[6] J. Akikusa, K. Adachi, T. Yamada, T. Akbay, N. Murakami, N. Chitose, K. Hoshino, K. Hosoi, H. Yoshida, T. Sasaki, T. Inagaki, T. Ishihara, Y. Takita, Development of a 1 kW class SOFC stack using doped lanthanum gallate, in: Proceedings of the Fifth European Solid Oxide Fuel Cell Forum, vol. 2, 1–5 July 2002, Lucerne, Switzerland, pp. 799–805.
[7] R. Chiba, T. Ishii, in: M. Dokiya, O. Yamamoto, H. Tagawa, S.C. Singhal (Eds.), Solid Oxide Fuel Cells IV, PV 95-1, The Electrochemical Society Proceedings Series, Pennington, NJ, 1995, p. 482.
[8] B. van Hassel, B. Boukamp, A. Burggraaf, Solid State Ionics 48 (1991) 139–154, and 155–171.
[9] S. Primdahl, M. Mogensen, in: U. Stimming, S.C. Singhal, H. Tagawa, W. Lehnert (Eds.), Solid Oxide Fuel Cells V, PV97-40, The Electrochemical Society Proceedings Series, Pennington, NJ, 1997, p. 530.
[10] T. Ishihara, T. Akbay, H. Furutani, Y. Takai, Solid State Ionics 113–115 (1998) 585–591.